Journal of Chemical and Petroleum Engineering 2020, 54(1): 111-128
DOI: 10.22059/jchpe.2020.292546.1301

RESEARCH PAPER

Mass Transfer Modeling of CO_2 Absorption into Blended MDEA-MEA Solution

Ahad Ghaemi*

School of Chemical, Gas and Petroleum Engineering, Iran University of Science and Technology, Narmak, Tehran, Iran

Received: 14 October 2019, Revised: 18 January 2020, Accepted: 28 April 2020

Abstract

In this research, the thermodynamics and mass transfer of CO_2 absorption has been studied in a mixture of MDEA-MEA amines. A relation is presented for mass transfer flux in the reactive-absorption process. For this purpose, the effective parameters on the mass transfer flux were investigated in both liquid and gas phases. Then, using dimensional analysis with the Pi-Buckingham theorem, the effective variables were extracted as the dimensionless parameters. Also, the absorption process with MEA-MDEA is modeled according to four laws of chemical equilibrium, phase equilibrium, mass, and charge balance (considering the appropriate thermodynamic model for solvent). The experimental data of the previous research was used to calculate the dimensionless parameters. The constants of the mass flux equation are calculated with the fitting method. Also, the effects of operating parameters such as CO_2 partial pressure, temperature, and dimensionless parameters such as the film parameter, enhancement factor, and loading have been investigated. The results showed that by increasing the loading and film parameter, the mass flux decreased, and the mean absolute error obtained from the proposed relationship was about 4.3%, which indicates the high accuracy of the predicted equation.

Keywords:
Buckingham Theorem,
Blended Amine MEA-MDEA,
Carbon Dioxide,
Mass Transfer Flux

Introduction

Energy plays a vital role in world economic growth. Climate change is essentially a worrying issue because of greenhouse gas emissions. Carbon dioxide (CO_2) accounts for about 78.1% of total greenhouse gas emissions. CO_2 removal from gas mixtures was used not only to remove sour gas but also to prevent greenhouse gas emissions. There are various methods such as physical and chemical absorption, adsorption, membrane technologies, cryogenic separation, etc. to remove CO_2 from gas mixtures, which energy consumption, removal efficiency, and process cost are the key aspects in the process selection [1-3]. The CO_2 capture from gas streams is a crucial step in many industrial processes, and this process is very important for technical, economic, and environmental reasons. In the presence of water, CO_2 becomes an acid gas that causes corrosion of the process equipment, and besides CO_2 reduces the thermal value of natural gas flow and wastes the pipeline capacity. Liquid gas plants should also be eliminated to prevent freezing in chillers at low temperatures and there is a possibility of catalyst poisoning in the production of ammonia [4].

One way to detect the need to sweeten sour gases is to calculate the partial pressures of acidic gases. Corrosion occurs at partial pressures greater than 30 psi and in the presence of water and

* Corresponding author:
Email: aghaemi@iust.ac.ir (A. Ghaemi)

carbon dioxide in the gas. In addition to the above, the operational problems arising from the presence of CO_2 in feedstuffs of chemical processes, the economic issues of large amounts of CO_2 through long-distance pipelines, as well as the sequestration and injection of CO_2 into the oilfields (Crude oil recycling) is important to prevent the impacts of greenhouse gas emissions on the Earth's atmosphere. Freezing CO_2 in natural gas liquefaction processes can block pipelines, heat exchangers, and other equipment [5]. One of the well-known methods is the use of aqueous solutions of alkanolamine, which is a proven and applicable method in many chemical processes such as ammonia production and natural gas processes [6-8]. In 1861, Woertz succeeded in obtaining alkanolamine by heating chlorohydrin and ammonia. In 1897, Knorr also obtained ethanolamine from ammonia and ethylene oxide [9]. In 1930, alkanolamines were first used to sweeten gas and have been used extensively but from 1970 due to their disadvantages such as corrosion and loss of monoethanolamine (MEA), solvent di-ethanolamine (DEA) replaced this amine. Since the middle of 1970, and especially in the last two decades, methyl-diethanolamine (MDEA) has gained widespread use in the gas industry because of its advantages such as the ability to selectively hydrogen sulfide in the presence of CO_2, high stability and low energy consumption for solvent recovery [10]. Recently, Piperazine (Pz), MEA-Pz, was used as a promoter and effective chemical solution for CO_2 absorption [11-12].

One of the most important factors in the absorption process is selecting the proper solvent that has a large impact on operating and investment costs. A good solvent should have high absorption capacity, high absorption rate, low recovery energy, and high stability. The advantages of the MEA solvent are its high reaction rate, low cost, low molecular mass, and low solubility of hydrocarbons. It also has disadvantages such as low CO_2 loading capacity, high recovery energy, and high viscosity. Recently, the use of a mixture of amines to remove CO_2 has attracted much attention. Mixing solvents is a useful technique for combining the advantages of each solvent in a new product. The mixture can adapt solvents with different physical and chemical properties to obtain better properties of each solvent alone [13]. The properties required to reduce energy consumption in the CO_2 removal technologies are achieved by employing mixtures of the first or second amines with the tertiary amines, such as the combination of MDEA and MEA. MED reacts with CO_2 more rapidly than MDEA. But MDEA has a higher absorption capacity than MEA. Also, MDEA needs less energy to recover than MED. Thus, in general, the advantage of MDEA, the third type of amine, over the first or second type amines, the high CO_2 loading capacity (mole of CO_2 per mole of amine), the low reaction temperature which results in less energy needed for recovery. By varying the ratio of the concentration of amines, an optimal absorption system can be designed for specific applications [1]. In 1985, Chakravarty et al. proposed a mixture of amines in which the advantages of each amine were obtained by adding a small amount of the first type of amine to the third amine. This mixture could improve the CO_2 absorption a large range without altering its properties [14]. Mixed-amine systems have become increasingly important in gas purification processes due to their increased use in the process design. In 2001, Mandal et al. investigated the CO_2 absorption in MDEA and MEA mixtures as well as amino-methyl-propanol (AMP) and MEA mixtures experimentally and numerically [15]. Mass transfer, reaction kinetics, and an equilibrium model were solved to describe CO_2 absorption in solvent mixtures. The results show that adding a small amount of MEA to the aqueous solution of MDEA significantly improves the rate of absorption and enhancement factor [1]. The solubility of CO_2 in the aqueous solution of MEA-MDEA was investigated at temperatures of 80 and 40°C for partial pressures lower than 315 kPa [16]. The solubility of CO_2 in the aqueous solution of MEA-MDEA has been experimentally studied for temperatures of 40-100 and partial pressures of more than 2000 kPa [17]. Table 1 provides a list of studies on absorption with the MEA-MDEA mixture solution.

Table 1. Review on studies of absorption process using aqueous solution of MEA-MDEA mixture

Author	Year	Concertation ratio MEA/MDEA	Temp. (K)	Loading	Ref.
Shen et al.	1992	12-24/18-6 (%wt)	313-373	0.1-1	[17]
AL-Ghawas et al.	1995	0.24-0.74/2.4-16.2 (kmol/m^3)	313	0	[18]
Mandal et al.	2001	0.24-0.74/2.14-2.4 (kmol/m^3)	313	0	[15]
Liao et al.	2002	0.1-0.5/1-1.5 (kmol/m^3)	303-313	0.0373-0.065	[19]
Lawal et al.	2005	5-7/2-2 (mol/L)	373-393	0.1-0.502	[20]
Ramanchandran et al.	2006	3-5-7/27-25-23 (%wt)	298-333	0.005-0.15	[13]
Ayandutan et al.	2006	2.5-1/9-1 (mol/L)	328-393	0.4-0.43	[21]
Edali et al.	2009	27-23/3-7(%wt)	298-333	0.005-0.15	[22]
Sema et al.	2012	2.3-2.1-1.95/0.5-0.8-1.16 (mol/L)	298-333	0.0097-0.14	[23]
Adeosun et al.	2013	10-25-40/40-25-10 (%wt)	313	0.5-0.99	[24]
Naami et al.	2013	2.3-2.1-1.95/0.5-0.8-1.16 (mol/L)	298-313	0.05-0.25	[25]

The previous researchers mainly investigated the CO_2 solubility in the MEA-MDEA system experimentally, as well as the kinetics of this system for temperature and loading ranges. Unfortunately, no exact models or exact equations to calculate the mass transfer flux have been obtained so far. So, calculating the height of the absorption columns or calculating the number of absorption trays in the reactive-absorption systems is inaccurate. The purpose of this study is to present a general and accurate method with the least simplifying assumptions for calculating the mass transfer flux of gas-to-liquid components in the MEA-MDEA electrolyte system.

Theory

Mass transfer with chemical reaction

Chemical absorption (reactive-absorption) is a process in which a gas is absorbed by the liquid phase through the mass transfer and reaction. Amine-based systems, carbonate-based systems, and ammonia-based systems and ionic liquids are chemical absorption systems. For CO_2 absorption, chemical absorption involves the reaction of CO_2 with a chemical solvent and an intermediate composition is formed with a weak bond with a reversible reaction [26]. This process is performed in different systems from the bubble absorbent column to the fixed-bed column. To dissipate the overall process rate, a liquid-gas contact layer has been developed and increased by increasing perturbation in both liquid and gas phases. At the boundary layer, the mass transfer occurs through a combination of diffusion and chemical reaction mechanisms. Thus, the overall process rate is expressed by both chemical reaction and mass transfer.

If the mass transfer is accompanied by a chemical reaction, the CO_2 absorption rate in the aqueous solution of amine is increased. Consequently, the mass transfer flux is obtained according to [27]:

$$N_A = \frac{1}{\frac{1}{E_A k_L} + \frac{R_T}{H k_G}} (C_A^* - C_{A,b}) \quad (1)$$

E_A is an enhancement factor that is defined as the ratio of the mass transfer coefficient with the reaction on the liquid bulk to the non-reaction mass transfer coefficient. For very low CO_2 loadings, the soluble concentration of CO_2 in the liquid bulk will be zero, resulting in the mass transfer flux [26]:

$$N_A = \frac{1}{\frac{1}{E_A k_L} + \frac{R_T}{H k_G}} (C_A^*) \quad (2)$$

Table 2. The relationships for enhancement factor in the reactive-absorption process.

Ref.	Author (Year)	Enhancement factor	Application
[29]	Wellek (1993)	$E_A = 1 + \frac{1}{[(E_{\inf}-1)^{-1.35} + (\frac{Ha}{\tan Ha}-1)^{-1.35}]^{1/1.35}}$ $Ha = \frac{\sqrt{k_2 D_{AL} C_{BL}}}{k_{AL}}$	Second-order irreversible reactions, Film theory model $A(g) + \upsilon_B B(L) \xrightarrow{k_2} product(L)$
[30]	Decoursey (1974)	$E = -\frac{Ha^2}{2(E_{\inf}-1)} + \sqrt{\frac{Ha^4}{4(E_{\inf}-1)^2} + \frac{E_{\inf} Ha^2}{(E_{\inf}-1)} + 1}$ $E_{\inf} = 1 + \frac{D_{BL} C_{BL}^{\delta}}{\upsilon_B D_{AL} C_{AL}^{*}}$	Second-order irreversible reaction, surface renewable model $A(g) + \upsilon_B B(L) \xrightarrow{k_2} product(L)$
[31]	Krevelen & Hoftijzer (1954)	$E = \frac{Ha\sqrt{\frac{(E_i - E)}{(E_i - 1)}}}{\tanh[Ha\sqrt{\frac{(E_i - E)}{(E_i - 1)}}]}$ $E_i = 1 + \frac{D_{BL}}{D_{AL}} \cdot \frac{C_{B\infty}}{z C_{AI}}$	Immediate reaction, Film model $A + zB \xrightarrow{k_2} z_p P$
[32]	Last et al. (2002)	$E = \frac{1}{1 - \frac{1/E_i}{(\frac{1}{Ha^{3/2}} + \frac{1}{E_i^{3/2}})^{2/3}}}$	Second-order irreversible reaction, Fast reaction
[33]	Wenmakers et al. (2016)	$E = \frac{1}{2}\sqrt{\pi k \tau}[(1 + \frac{1}{2k\tau})erf(\sqrt{k\tau}) + \frac{\exp(-k\tau)}{\sqrt{\pi k \tau}}]$	Fixed bed column with catalytic particles and immediate reaction
[34]	Hikita & Asia (1964)	$E = (\sqrt{M(\frac{E_a - E}{E_a - 1})} + \frac{\pi}{8} / \sqrt{M(\frac{E_a - E}{E_a - 1})}) \times$ $erfc\sqrt{\frac{4}{\pi} M(\frac{E_a - E}{E_a - 1})} + \frac{1}{2}\exp[-\frac{4}{\pi} M(\frac{E_a - E}{E_a - 1})]$	The pseudo-first-order reaction, Higbie diffusion theory
[35]	Bokotko et al. (2005)	$E = 1 + \sqrt{D_{HSO_3^-} K_{HSO_3^-} / D_{SO_2}} / (\sqrt{C_{SO2,L}} + \sqrt{C_{SO2}})$	SO_2 absorption into an aqueous solution in a bubble column with NH_4HCO_3-immediate irreversible reaction based on surface renewable theory $A + YB \rightarrow Product$
[36]	Li et al. (1982)	$E = \frac{(Y_1^2 - Y_2^2)(\frac{1}{1+K_{13}})}{(1 - ZY_2^2)\frac{\tanh(Y_1\sqrt{M})}{Y_1\sqrt{M}} - (1 - ZY_1^2)\frac{\tanh(Y_2\sqrt{M})}{Y_2\sqrt{M}}} +$ $(\frac{1}{1+K_{13}} - Z)(Y_1^2 - Y_2^2)$ $M = \frac{K_{12} L^2}{D_1}$	First-order reversible reaction or pseudo-first-order reaction based on film theory
[37]	Sun et al. (2004)	$E = \sqrt{\frac{D_{CO_2}}{D_{amine}}} + \frac{[amine]}{z[CO_2]_i}\sqrt{\frac{D_{amine}}{D_{CO_2}}}$	Pseudo-first-order immediate reaction based on surface renewable theory

[38]	Van Swaiji & Versteeg (1993)	$E = Ha[\{1+\frac{\pi}{8Ha^2}erf\ [\sqrt{\frac{4Ha^2}{\pi}}]+\frac{1}{2Ha}\exp(\frac{4Ha^2}{\pi})\}]$	Pseudo-first-order irreversible reaction

If pure CO_2 was used, the mass transfer resistance in the gas phase is negligible. Consequently, the mass transfer flux [26]:

$$N_A = E_A k_L C_A^* \tag{3}$$

E_A will be an effective parameter when the mass transfer is coupled with chemical reaction. The enhancement factor can be calculated based on mass transfer models such as surface renewable model, film theory, and penetration theory [28]. Table 2 shows the relationships for the calculation of the enhancement factor provided by different researchers.

Dimensional analysis for reactive-absorption process

In the reactive-absorption process, mass transfer flux is dependent on the variables below.

$$N_A = f\ (k, k_L, D_G, D_L, \delta_G, \delta_L, P_{CO_2}, P_t, C_{CO_2}, C_{Am}) \tag{4}$$

In Table 3, all variables with their dimensions are presented [39].

Table 3. Dependent variables in mass transfer flux with their dimensions

Parameter	Definition	Dimension	Unit
N_A	Mass transfer flux	$ML^{-2}T^{-1}$	$mol/(m^2.s)$
k	Reaction constant	$L^3M^{-1}T^{-1}$	$m^3/(mol.s)$
k_L	Mass transfer coefficient of liquid phase	LT^{-1}	m/s
D_G	Mass transfer coefficient of gas phase	L^2T^{-1}	m^2/s
D_L	CO_2 diffusion coefficient in liquid	L^2T^{-1}	m^2/s
δ_G	Gas film thickness	L	m
δ_L	Liquid film thickness	L	m
P_{CO_2}	CO_2 partial pressure in gas phase	$ML^{-1}T^{-2}$	Pa
P_t	Total pressure	$ML^{-1}T^{-2}$	Pa
C_{CO_2}	CO_2 concentration	ML^{-3}	mol/m^3
C_{Am}	Amine concentration	ML^{-3}	mol/m^3

Number of main dimensions: k=3 (M, L, T)
Number of variables: n=11
So, p=n-k=11-3=8;

In this case, 8 dimensionless number must be defined. Based on Buckingham-π theorem, the number of main variables is assumed to be equal to the number of main dimensions. The considered main variables in the current study are D_L, δ_L, C_{CO2}. Thus, the dimensionless groups are represented in Table 4 and dimensionless numbers used in the present study are presented in Table 5.

Table 4. The dimensionless groups obtained in CO_2 absorption process.

Group No.	Dimensionless group	Group No.	Dimensionless group
π_1	$D_L^a \delta_L^b C_{CO_2}^c . N_A$	π_5	$D_L^m \delta_L^n C_{CO_2}^o . \delta_G$
π_2	$D_L^d \delta_L^e C_{CO_2}^f . k_L$	π_6	$D_L^p \delta_L^q C_{CO_2}^r . P_{CO_2}$
π_3	$D_L^g \delta_L^h C_{CO_2}^i . k$	π_7	$D_L^s \delta_L^t C_{CO_2}^u . P_t$
π_4	$D_L^j \delta_L^k C_{CO_2}^l . D_G$	π_8	$D_L^v \delta_L^w C_{CO_2}^x . C_{Am}$

Table 5. The dimensionless number obtained based on Buckingham-π theorem [39]

No.	Description	Dimensionless Number
1	Enhancement factor: Ratio of absorbed amount with chemical reaction to one without chemical reaction	$E_A = \frac{N_A}{k_L C_{CO_2}}$
2	Sherwood: Ratio of mass transfer with convention mechanism to one with diffusion mechanism	$sh = \frac{k_L}{\delta_L D_L}$
3	Film parameter: Ratio of maximum film conversion to maximum diffusion rate through the film	$M^2 = \frac{k C_{Am} C_{CO_2} \delta_L}{k_L C_{CO_2}}$
4	Loading: Ratio of CO_2 absorbed amount to amine mole	$\alpha = \frac{C_{CO_2}}{C_{Am}}$
5	Ratio of film thickness of gas to liquid	$\frac{\delta_G}{\delta_L}$
6	Ratio of CO_2 partial pressure in gas phase to total pressure	$\frac{P_{CO_2}}{P_t}$
7	Ratio of CO_2 diffusion coefficient in gas phase to liquid phase	$\frac{D_G}{D_L}$

Film parameter indicates the effects of reaction on mass transfer in the boundary layer near the interface. From the Buckingham-π theorem:

$$\pi_1 = f\ (\pi_2, \pi_3, \pi_4, ...\pi_7) \tag{5}$$

$$\frac{N_A}{k_L (C^* - C)} = f\ (Sh, \frac{P_{CO_2}}{P_t}, \frac{D_g}{D_L}, \frac{\delta_g}{\delta_L}, M, \alpha) \tag{6}$$

And consequently:

$$\frac{N_A}{k_L (C^*_{CO_2} - C_{CO_2,b})} = A.(Sh)^a (M.\alpha)^b (\frac{D_G}{D_L})^c (\frac{\delta_G}{\delta_L})^d (\frac{P_{CO_2}}{P_t})^e (\frac{1}{\alpha})^f \tag{7}$$

Where the coefficient of the above equation depends on operating conditions and solvent type. By simplifying the Eq. 7:

$$\frac{N_A}{k_L (C^*_{CO_2} - C_{CO_2,b})} = A.(Sh)^a (M)^b (\frac{D_G}{D_L})^c (\frac{\delta_G}{\delta_L})^d (\frac{P_{CO_2}}{P_t})^e \alpha^g \tag{8}$$

Since the film model is assumed in the present study and the Sherwood number will be equal to 1 [39].

$$\frac{N_A}{k_L(C^*_{CO_2}-C_{CO_2,b})}=A.(\alpha)^F(\frac{D_G}{D_L})^E(\frac{\delta_G}{\delta_L})^D(\frac{P_{CO_2}}{P_t})^C M^B \quad (9)$$

The unknown parameters are the coefficient of A, B… F. Eq. 9 is the mass transfer flux correlation which is true in the CO_2 absorption process and is independent of the solvent type and operating conditions.

Vapor-liquid equilibrium modeling

Acidic gases and alkanolamines are weak electrolytes that are partially decomposed in the liquid phase to form a complex mixture of volatile and relatively volatile solvent, high volatility molecular components (such as CO_2), and non-volatile ionic components. In a closed system at constant temperature and pressure, the fuzzy equilibrium produces the distribution of molecular components between the vapor and liquid phases, while the chemical reaction in the liquid phase occurs between the acidic gas and the alkanolamines to produce ionic components. The chemical and fuzzy equilibrium are effectively coupled with this system. As a result, the degradation degree of the weak liquid phase electrolytes is affected by the partial pressure of the acidic gas in the vapor phase. Hence the expression of the vapor-liquid equilibrium behavior of acid-alkanolamine-water gas systems is complicated due to the large number of chemical reactions occurring in the system. Therefore, the expression of fuzzy equilibrium for such systems requires consideration of both fuzzy and chemical equilibrium. VLE models play an important role in simulating water-alkanolamine-acid gas systems. In the equilibrium state of liquid and vapor phases for weak electrolyte solutions, the thermodynamic analysis of the phase equilibrium of these solutions is based on the four laws of mass balance, charge balance, chemical equilibrium, and fuzzy equilibrium. In these systems, usually, the amine vapor pressure is very low, so the presence of amines and ions in the vapor phase is negligible. Following is the modeling of the MDEA-MEA-CO_2-H_2O electrolyte system. The following reactions occur when CO_2 is absorbed in the MEA-MDEA solution, according to Rinker et al. and Versteeg et al. [13]:

$$H_2O \xleftrightarrow{K_1} OH^- + H^+ \quad (10)$$

$$CO_2 + H_2O \xleftrightarrow{K_2} HCO_3^- + H^+ \quad (11)$$

$$HCO_3^- \xleftrightarrow{K_3} CO_3^{2-} + H^+ \quad (12)$$

$$MDEA + H^+ \xleftrightarrow{K_4} MDEAH^+ \quad (13)$$

$$MEA + CO_2 \xleftrightarrow{K_5} MEACOO^- + H^+ \quad (14)$$

$$MEA + H^+ \xleftrightarrow{K_6} MEAH^+ \quad (15)$$

Chemical Equilibrium

The equilibrium constants for the equations mentioned in the previous section can be determined using Eq. 16 and information of Table 6 [13].

$$LnK = A + \frac{B}{T} + CLnT \quad (16)$$

Mass and charge balances

Mass balances for MDEA, MEA, and CO_2 are as follow [40]:

$$m_{MEA,i} = m_{MEA} + m_{MEACOO^-} + m_{MEAH^+} \quad (17)$$

$$m_{MDEA,i} = m_{MDEA} + m_{MDEAH^+} \quad (18)$$

$$\alpha(m_{MEA} + m_{MDEA}) = m_{CO_2} + m_{HCO_3^-} + m_{CO_3^{2-}} + m_{MEACOO^-} \quad (19)$$

Table 6. Parameters of chemical equilibrium constant equation for MDEA-MEA-CO_2-H_2O system [13]

Equation	A	B	C
(10)	132.89	-13446	-22.47
(11)	231.465	-12092.1	-36.7816
(12)	216.04	-12431.7	-35.4819
(13)	-9.416	-4234.98	-
(14)	2.8898	-3635.09	-
(15)	2.1211	-8189.38	-0.007484

Charge balance [40]:

$$m_{H^+} + m_{MEAH^+} + m_{MDEAH^+} = m_{OH^-} + m_{HCO_3^-} + 2m_{CO_3^{2-}} + m_{MEACOO^-} \quad (20)$$

In this system, the expanded UNIQUAC model is used to model the liquid phase and calculate the activity coefficient of molecules and ions. This is a mode based on activity coefficient for electrolyte systems that the excess Gibbs free energy is given as [41]:

$$G^{Excess} = G^{Excess}_{Combinatorial} + G^{Excess}_{Residual} + G^{Excess}_{Debye-Huckel} \quad (21)$$

Two first terms are the combined and residual terms indicating short-range and the last term represents the long-range of ion-ion that are calculated from the Debye-Huckel correlation. The equation of combined activity coefficient is presented as following [40]:

$$Ln\gamma_i^C = Ln(\frac{\phi_i}{x_i}) + 1 - \frac{\phi_i}{x_i} - \frac{z}{2}q_i[Ln(\frac{\phi_i}{\theta_i}) + 1 - \frac{\phi_i}{\theta_i}] \quad (22)$$

And for residual terms [40,41]:

$$Ln\gamma_i^R = q_i[1 - Ln(\sum_j \theta_j \psi_{ji}) - \sum_j (\frac{\theta_j \psi_{ij}}{\sum_k \theta_k \psi_{kj}})] \quad (23)$$

$$\phi_i = \frac{x_i r_i}{\sum_j x_j r_j} \quad (24)$$

$$\theta_i = \frac{x_i q_i}{\sum_j x_j q_j} \quad (25)$$

$$\psi_{ji} = \exp(\frac{u_{jj} - u_{ij}}{T}) \quad (26)$$

Where r_i and q_i are the volume and are of component i which for the studied system are presented in Table 7. u_{ij} and u_{jj} are the energy interaction parameters as calculated below [40].

$$u_{ij} = u_{ij}^0 + u_{ij}^T (T - 298.15) \quad (27)$$

Table 7. Values of r and q for the MDEA-MEA-CO_2-H_2O system [40].

component	r	q
MDEA	0.13445	0.54315
$MDEAH^+$	2.3931	1.0749
H_2O	0.92	1.4
MEA	4.28	4.28
CO_2	5.741	6.0806
H_3O^+	0.13779	10^{-15}
$MEAH^+$	1.0241	2.515
OH^-	9.3973	8.8171
HCO_3^-	8.0756	8.6806
CO_3^{2-}	1.828	10.769
$MEACOO^-$	1.0741	0.1106

Also, the values of the interaction parameter are presented in Table 8 and Table 9. By putting x_w=1 in Eqs. 22 and 23, the equations in infinite dilution conditions will be obtained as following [41, 40]:

$$Ln\gamma_i^{C\infty} = Ln(\frac{r_i}{r_w}) + 1 - \frac{r_i}{r_w} - \frac{z_i}{2} q_i [Ln(\frac{r_i q_w}{r_w q_i}) + 1 - \frac{r_i q_w}{r_w q_i}] \quad (28)$$

$$Ln\gamma_i^R = q_i (1 - Ln\psi_{wi} - \psi_{iw}) \quad (29)$$

Similarly, by deriving the excess Gibbs free energy equation as a function of the Debye-Huckel term, the electrostatic force term is calculated as following [40,41]:

$$Ln\gamma_i^{*DH} = -Z_i^2 \frac{A\sqrt{I}}{1+b\sqrt{I}} \quad (30)$$

$$Ln\gamma_w^{DH} = M_w \frac{2A}{b^3}[1+b\sqrt{I} - \frac{1}{1+b\sqrt{I}} - 2Ln(1+b\sqrt{I})] \quad (31)$$

The Debye-Huckel parameter [41]:

$$A = [1.131 + 1.335\times10^{-3}(T - 273.15) + 1.164\times10^{-5}(T - 273.15)^2](kg.mol^{-1})^{1/2} \quad (32)$$

b is a constant with a value of 1.5 $(kg.mol^{-1})^{1/2}$ and I is the ionic strength. Finally, the activity coefficient for the molecular and ionic components in the form of Eq. 33, which will be a set of three combined, residual, and Debye-Huckel terms [42].

$$Ln\gamma_i^* = Ln(\frac{\gamma_i^c}{\gamma_i^{c\infty}}) + Ln(\frac{\gamma_i^R}{\gamma_i^{R\infty}}) + Ln\gamma_i^{*DH} \quad (33)$$

Also, the activity coefficient of water is determined as follow:

$$Ln\gamma_w = Ln\gamma_w^c + Ln\gamma_w^R + Ln\gamma_w^{DH} \quad (34)$$

In the MDEA-MEA solution, the reaction rate equation is [41,43]:

$$R_{CO_2} = k_{MDEA,CO_2} C_{MDEA} (C^*_{CO_2} - C_{CO_2,b}) + k_{MEA,CO_2} C_{MEA} (C^*_{CO_2} - C_{CO_2,b}) + k_{OH,CO_2} (C^*_{CO_2} - C_{CO_2,b}) \quad (35)$$

$$k_{MDEA}(m^3 kmol^{-1} s^{-1}) = 4.01\times10^8 \exp[-\frac{5400}{T}] \quad (36)$$

Table 8. Parameters of energy interaction u_{ij}^{0} for the MDEA-MEA-CO_2-H_2O system [40].

u_{ij}^{T}	**H_2O**	**MEA**	**CO_2**	**H_3O^+**	**$MEAH^+$**	**OH^-**	**HCO_3^-**	**CO_3^{2-}**	**$MEACOO^-$**	**MDEA**	**$MDEAH^+$**
H_2O	0	0.803	6.091	0	-1.917	8.5455	6.950	3.3516	16.9192	0.10616	-0.00359
MEA	0.803	0.665	4.666	0	0.1213	0	15.2488	0	0	0	0
CO_2	6.091	4.666	13.63	0	7.3541	0	5.8077	0	0	0	9.473
H_3O^+	0	0	0	0	0	0	0	0	0	0	0
$MEAH^+$	-1.917	0.1213	7.3541	0	0	0	2.8863	0	0	0	0
OH^-	8.5455	0	0	0	0	5.6169	0	2.7496	0	0	0
HCO_3^-	6.950	15.2488	5.8077	0	2.8863	0	17.1148	2.6115	0	0	0
CO_3^{2-}	3.3516	0	0	0	0	2.75	2.6115	-1.3448	0	0	0
$MEACOO^-$	16.9192	0	0	0	0	0	0	0	0	0	0
MDEA	0.10616	0	0	0	0	0	0	0	0	-2.637	0
$MDEAH^+$	-0.00359	0	9.473	0	0	0	0	0	0	0	0

Table 9. Parameters of energy interaction u_{ij}^{T} for the MDEA-MEA-CO_2-H_2O system [40].

u_{ij}^{0}	**H_2O**	**MEA**	**CO_2**	**H_3O^+**	**$MEAH^+$**	**OH^-**	**HCO_3^-**	**CO_3^{2-}**	**$MEACOO^-$**	**MDEA**	**$MDEAH^+$**
H_2O	0	173.96	-151.46	104	-20.77	600.495	517.028	361.69	2758.38	-561.67	-294.39
MEA	173.96	414.69	87.556	10^9	310.13	10^9	655.09	10^9	10^9	0	0
CO_2	-151.46	87.56	40.5176	10^9	30.8035	2500	597.97	2500	10^9	10^9	-742.52
H_3O^+	10^4	10^9	10^9	0	10^9	10^9	10^9	10^9	10^9	10^{10}	10^{10}
$MEAH^+$	-20.77	310.13	30.8035	10^9	0	10^9	732.7	10^9	10^9	0	0
OH^-	600.495	10^9	2500	10^9	10^9	1562.9	2500	1588.02	10^9	10^{10}	10^{10}
HCO_3^-	517.028	655.09	597.97	10^9	732.7	2500	743.62	719.16	10^9	10^{10}	10^{10}
CO_3^{2-}	361.39	10^9	2500	10^9	10^9	1588.02	719.16	1458.34	10^9	10^{10}	10^{10}
$MEACOO^-$	2758.38	10^9	10^9	10^9	10^9	10^9	10^9	10^9	1500	0	0
MDEA	-561.67	0	10^9	10^{10}	0	10^{10}	10^{10}	10^{10}	0	-1489.8	10^{10}
$MDEAH^+$	-294.39	0	-764.52	10^{10}	0	10^{10}	10^{10}	10^{10}	0	10^{10}	0

$$k_{MEA}(m^3 kmol^{-1}s^{-1}) = 7.973\times10^{12}\exp[-\frac{6243}{T}] \quad (37)$$

$$\log_{10}(k^*_{OH^-}/m^3 kmol^{-1}s^{-1}) = 13.635 - \frac{2895}{T} \quad (38)$$

CO_2 Concentration Absorbed in the Liquid Bulk

Four laws of mass balance, chemical equilibrium, and fuzzy equilibrium as well as the activity coefficient equations using the UNIQUAC thermodynamic model are solved numerically to calculate the CO_2 concentration in the liquid block. It should be noted that the overall concentrations of MEA and MDEA, loading, and temperature are considered as input variables.

CO_2 Concentration Absorbed at the Interface

In this section, the same equations will be given for the bulk concentration calculation section, but the equation of thermodynamic equilibrium in the gas-liquid interface is also added to them. This equation presented in the following [11].

$$H_{CO_2,H_2O}\exp(\frac{V^{\infty}_{CO_2}(P-P^{sat}_w)}{RT})a_{CO_2} = y_{CO_2}P_t\varphi_{CO_2} \quad (39)$$

Film Parameter

The CO_2 concentrations in the liquid bulk and interface and reaction rate are used to calculate the film parameter. It should be noted that the experimental data used in the previous researches to calculate the dimensionless parameters which their operating conditions are presented in Table 10 [44].

Table 10. Operating conditions in the MDEA-MEA solution [44]

Solvent concentration (MEA/MDEA)	Loading mol CO_2/mol (amine	CO_2 partial pressure (Pa)	Total pressure (Pa)	Temperature (°C)
9.8-3.4	0.249-0.438	91-35000	10325	20-100

Consequently, the constants of Eq. 9 are obtained using nonlinear regression and the mass transfer flux equation for MDEA-MEA solution is presented in Eq. 40.

$$N_{CO_2} = 0.0225k_L(C^*_{CO_2} - C_{CO_2,b})\alpha^{-9.52}(\frac{P_{CO_2}}{P_t})^{1.358}(\frac{\delta_G}{\delta_L})^{0.732}(\frac{D_G}{D_L})^{0.5636}M^{-0.741} \quad (40)$$

Numerical Solution

The Nelder-Mead method was employed for the determination of the correlation coefficients. The Nelder-Mead algorithm has become one of the most widely used methods for nonlinear unconstrained optimization [34]. It is especially popular in the fields of chemistry and chemical engineering. The Nelder-Mead method attempts to minimize a nonlinear function of N real variables using only function values, without any derivative information. It is a heuristic search method that can converge to non-stationary points on problems that can be solved by alternative methods. The method approximates a local optimum when the objective function varies smoothly and is unimodal. In the present work, Eq. 9 is changed to the following form [45]:

$$N_A(x_1,...,x_k) = \beta_1.x_1(x_2)^{\beta_2}(x_3)^{\beta_3}(x_4)^{\beta_4}(x_5)^{\beta_5}(x_6)^{\beta_6} \quad (41)$$

Where, $x_1 = k_L(C^*_{CO_2} - C_{CO_2,b})$, $x_2 = \alpha$, $x_3 = P_{CO_2}/P_t$, $x_4 = \delta_G/\delta_L$, $x_5 = D_G/D_L$, $x_6 = M$.

The values of $\beta_1,...,\beta_6$ are obtained by minimizing the quantity $\sum_{i=1}^{n} e_i^2$, where e_i is given by:

$$e_i = N_{A,\exp} - N_A(x_1,...,x_k) = N_{A,\exp} - \left(\beta_1 . x_1 (x_2)^{\beta_2} (x_3)^{\beta_3} (x_4)^{\beta_4} (x_5)^{\beta_5} (x_6)^{\beta_6}\right) \quad (42)$$

The objective function which is used to find β_i's is mean squared error (MSE):

$$MSE = \frac{\sum_{i=1}^{n} e_i^2}{n-p} \quad (43)$$

Where n is the number of experimental data and p is the number of β parameters.

Results and Discussions

In this study, the CO_2 mass transfer flux using Buckingham-π theorem is equated as a function of dimensionless parameters of film parameter, loading, gas-liquid diffusion coefficient ratio, gas-liquid film thickness ratio, and partial pressure-to-total pressure ratio. Then the MEA - MDEA mixed solution system was modeled and finally, the equation constants were calculated using non-linear regression. In Fig. 1, the mass transfer flux is shown at different loadings and film parameters. As it is obvious that the lower loading causes lower CO_2 content in the solvent and result in increasing the driving force (concentration difference) leading to the mass transfer flux increment. It is also observed that by increasing the film parameter, the mass transfer flux decreases and the slope of the mass transfer curve decreases relative to the loading one. In fact, in the higher film parameters, the film parameter has less influence on the mass transfer flux. Fig. 2 depicts a 3D plot of the variation of mass transfer flux versus loading and film parameter.

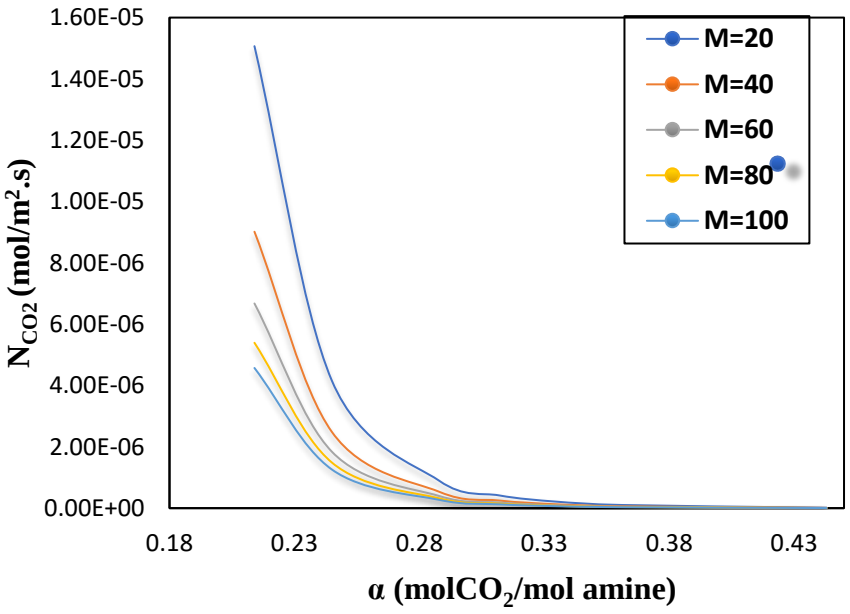

Fig. 1. Mass transfer flux versus loading at different film parameters.

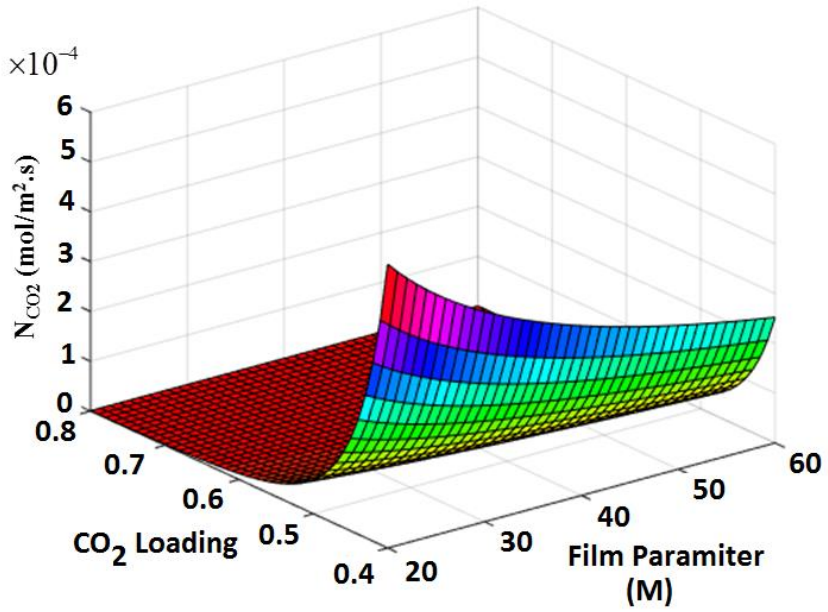

Fig. 2. 3D plot of the variation of mass transfer flux versus film parameter and loading.

The mass transfer flux in terms of the ratio of partial pressure to total pressure at different loadings is illustrated in Fig. 3, as it is evident that as the CO_2 partial pressure increases, the mass transfer driving force and the mass transfer flux increase. Also, as the loading increases, the free amine concentration decreases leading to a decrease in the mass transfer flux. It is clear that at lower CO_2 loading the slopes are higher so, the mass transfer flux is higher.

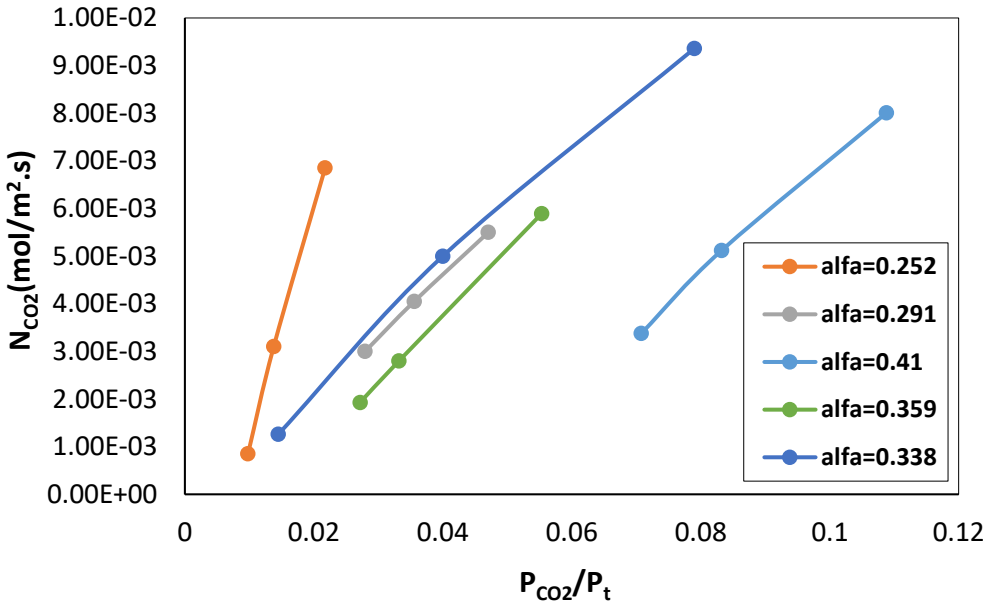

Fig. 3. Variation mass transfer flux relative to partial pressure at different loadings.

In Fig. 4, the enhancement factor versus the film parameter is plotted at different temperatures. As can be observed, by increasing the temperature the slope of the enhancement factor decreases, indicating that the adsorption process is slower at higher temperatures. Also, at higher temperatures, the rate of enhancement factor decreases, and since this factor is proportional to the mass transfer flux, so the mass transfer flux decreases with enhancing the temperature. This is obvious because the adsorption process is often exothermic and as the temperature increases, the mass transfer flux decreases.

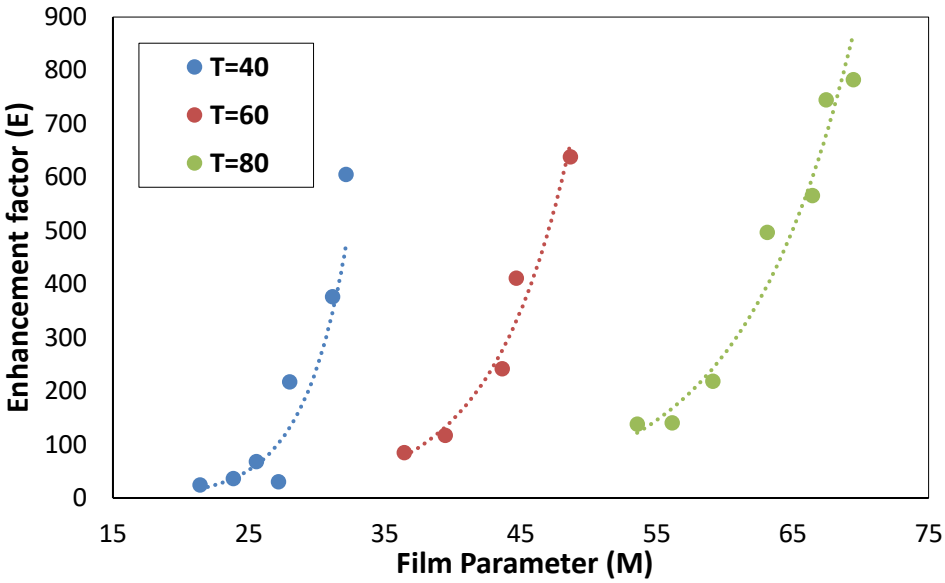

Fig. 4. Variation of enhancement factor versus film parameter at different temperatures.

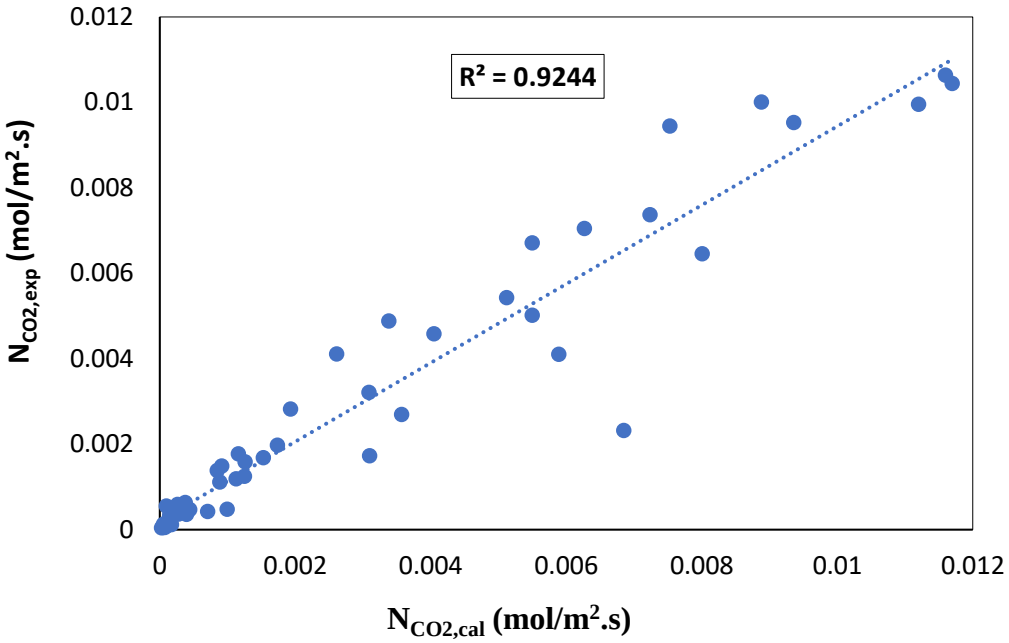

Fig. 5. Comparison of experimental and predicted mass transfer flux.

Finally, the experimental data of the mass transfer flux were compared with the predicted mass transfer flux and the correlation coefficient of 0.9244 was obtained. Also, the relative average error was 4.8%. Fig. 5 shows the experimental versus predicted values for mass transfer flux. Also, in Fig. 6, the concentration of the ionic components is shown versus loading values.

Table 11 compares the amount of deviation of the mass transfer flux from the obtained value with the previous research. As shown, the present correlation has the least deviation in comparison with the previous researches. This indicates the high accuracy of the predicted correlation.

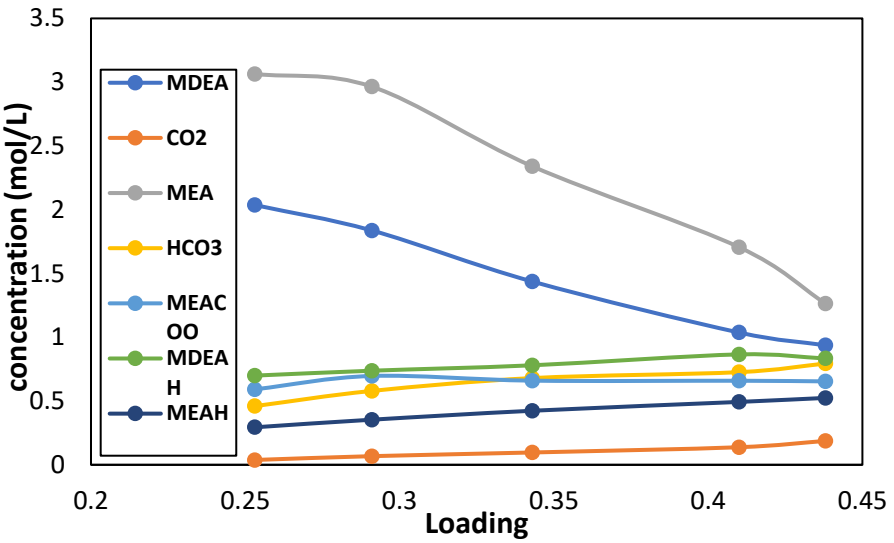

Fig. 6. The concentration of Ionic components in the MDEA-MEA solution.

Table 11. Comparison of the deviation of the present correlation and previous researches.

Researchers	Deviation (%)	Reference
Mandal et al. (2001)	5	[15]
Edali et al. (2010)	7.76	[4]
Puxty et al. (2011)	15	[46]
Samanta et al. (2002)	6.8	[47]
Eq. 40	4.8	Present work

Conclusion

To design and simulate gas treatment processes involving amine hybrid solvents, it is necessary to develop mass transfer rate-based models to describe the mass transfer of CO_2 in these solvents. In the current study, the parameters affecting the mass transfer flux were obtained and using Buckingham-π theorem, the mass transfer flux correlation as a function of dimensionless variables (film parameter, gas diffusion coefficient to liquid diffusion coefficient, gas to liquid film thickness ratio, CO_2 partial pressure to total pressure, and loading) and liquid mass transfer coefficient and mass transfer driving force were expressed. It should be noted that the presented correlation is general and applicable to different absorption conditions. The behavior of the absorption process was then modeled according to the laws of chemical equilibrium, phase equilibrium, mass, and charge balances. All reactions occurring in the liquid phase are also taken into account. To calculate some thermodynamic properties such as activity coefficient, the UNOQUAC thermodynamic model was used. The behavior of some of the operating parameters was investigated to check the accuracy of the correlation results. As shown in the equations, this parameter has a negative coefficient indicating its negative effects on the mass transfer flux. Because of the lower the initial loading, the lower CO_2 content of the solvent leading to the higher adsorption capacity and mass transfer flux. The error percentage of the predicted values for the electrolyte system was calculated, as it is evident that the correlation values are highly accurate.

Nomenclature

$C_{CO_2}(mol/L)$	CO_2 concetration in liquid bulk	$N_{CO_2}(mol/m^2.s)$	CO_2 mass transfer flux
$k_L^0(m/s)$	Liquid phase mass transfer coefficient	$C_{CO_2}^*(mol/L)$	CO_2 concentration at interface

$P_t\,(Pa)$	Total pressure	$H_{CO_2}\,(Mpa.kg\,/\,mol)$	CO2 Henry's constant
$P_w^{sat}\,(Pa)$	Water's saturated vapor pressure	$P_{CO_2}\,(Pa)$	CO_2 partial pressure
$D_L\,(m^2\,/\,s)$	Liquid phase diffusion coefficient	$D_g\,(m^2\,/\,s)$	Gas phase diffusion coefficient
$C_{Am}\,(mol\,/\,L)$	Amine concentration	$r_{CO_2}\,(mol\,/\,L.s)$	CO_2 reaction rate
r_i	Volume parameter	$I\,(mol\,/\,kg)$	Ionic strength
q_i	Surface area parameter	$A_Q\,(kg\,/\,mol)^{1/2}$	Debye-Huckel parameter
$T\,(k)$	Temperature	$B_{i,j}\,(cm^3\,/\,mol)$	Second Virial coefficient between i, j
Sh	Sherwood Number	E	Enhancement factor
u_{ij}	Binary interation of i,j	M	Film parameter
y_{CO_2}	CO_2 mole fraction in gas phase	$k\,(m^3\,/\,mol.s)$	Reaction constant
Z	Ion charge	K	Chemical equilibrium constant
α	Loading	$M_w\,(kg\,/\,mol)$	Water molecular weight
$\delta_L\,(m)$	Liquid film thickness	$\delta_g\,(m)$	Gas film thickness
γ_i	Activity coefficient of species i	β_{ij}	Binary interaction coefficient
ϕ_i	Volume fraction of species i	θ_i	Surface fraction of species i
τ_{ijk}	Tertiary interaction coefficient	λ_{ij}	Second Virial coefficient

References

[1] Naami A. Mass transfer studies of carbon dioxide absorption into aqueous solutions of 4-(diethylamine)-2-butanol, blended monoethanolamine with 4-(diethylamine)-2-butanol, and blended monoethanolamine with methyldiethanolamine. [Doctoral dissertation]. Regina: University of Regina; 2013.

[2] Khajeh M, Ghaemi A. Exploiting response surface methodology for experimental modeling and optimization of CO_2 adsorption onto NaOH-modified nanoclay montmorillonite. Journal of Environmental Chemical Engineering. 2020 Apr 1;8(2):103663.

[3] Ramezanipour Penchah H, Ghaemi A, Ganadzadeh Gilani H. Benzene-based hyper-cross-linked polymer with enhanced adsorption capacity for CO_2 capture. Energy & Fuels. 2019 Nov 6;33(12):12578-86.

[4] Edali M, Idem R, Aboudheir A. 1D and 2D absorption-rate/kinetic modeling and simulation of carbon dioxide absorption into mixed aqueous solutions of MDEA and PZ in a laminar jet apparatus. International Journal of Greenhouse Gas Control. 2010 Mar 1;4(2):143-51.

[5] Pashaei H, Zarandi MN, Ghaemi A. Experimental study and modeling of CO_2 absorption into diethanolamine solutions using stirrer bubble column. Chemical Engineering Research and Design. 2017 May 1;121:32-43.

[6] Kazemi S, Ghaemi A, Tahvildari K. Chemical absorption of carbon dioxide into aqueous piperazine solutions using a stirred reactor. Iranian Journal of Chemistry and Chemical Engineering (IJCCE). 2019 May 11.

[7] Ghaemi A, Jafari Z, Etemad E. Prediction of CO_2 mass transfer flux in aqueous amine solutions using artificial neural networks. Iranian Journal of Chemistry and Chemical Engineering (IJCCE). 2018 Jul 18.

[8] Pashaei H, Zarandi MN, Ghaemi A. Experimental study and modeling of CO_2 absorption into diethanolamine solutions using stirrer bubble column. Chemical Engineering Research and Design. 2017 May 1;121:32-43.

[9] Campbell JM, and Maddox RN, Gas conditioning and processing vol. 1: The Basic Principles. Campbell Petroleum Series, 1970.
[10] Kohl AL, and Nielsen R. Gas purification: Gulf Professional Publishing, 1997.
[11] Pashaei H, Ghaemi A, Nasiri M. Experimental investigation of CO_2 removal using Piperazine solution in a stirrer bubble column. International Journal of Greenhouse Gas Control. 2017 Aug 1;63:226-40.
[12] Mirzaei F, Ghaemi A. An experimental correlation for mass transfer flux of CO_2 reactive absorption into aqueous MEA-PZ blended solution. Asia-Pacific Journal of Chemical Engineering. 2018 Nov;13(6):e2250.
[13] Ramachandran N, Aboudheir A, Idem R, Tontiwachwuthikul P. Kinetics of the absorption of CO_2 into mixed aqueous loaded solutions of monoethanolamine and methyldiethanolamine. Industrial & Engineering Chemistry Research. 2006 Apr 12;45(8):2608-16.
[14] Chakravarty T, Phukan UK, Weilund RH. Reaction of acid gases with mixtures of amines. Chemical Engineering Progress;(United States). 1985 Apr 1;81(4).
[15] Mandal BP, Guha M, Biswas AK, Bandyopadhyay SS. Removal of carbon dioxide by absorption in mixed amines: modelling of absorption in aqueous MDEA/MEA and AMP/MEA solutions. Chemical Engineering Science. 2001 Nov 1;56(21-22):6217-24.
[16] Austgen DM, Rochelle GT, Chen CC. Model of vapor-liquid equilibria for aqueous acid gas-alkanolamine systems. II, Representation of H2S and CO_2 solubility in aqueous MDEA and CO_2 solubility in aqueous mixtures of MDEA qwith MEA or DEA. Industrial & Engineering Chemistry Research. 1991;30(3):543-55.
[17] Shen KP, Li MH. Solubility of carbon dioxide in aqueous mixtures of monoethanolamine with methyldiethanolamine. Journal of chemical and Engineering Data. 1992 Jan;37(1):96-100.
[18] Hagewiesche DP, Ashour SS, Al-Ghawas HA, Sandall OC. Absorption of carbon dioxide into aqueous blends of monoethanolamine and N-methyldiethanolamine. Chemical Engineering Science. 1995 Apr 1;50(7):1071-9.
[19] Norouzbahari S, Shahhosseini S, Ghaemi A. Chemical absorption of CO 2 into an aqueous piperazine (PZ) solution: development and validation of a rigorous dynamic rate-based model. RSC Advances. 2016;6(46):40017-32.
[20] Lawal AO, Idem RO. Effects of Operating Variables on the Product Distribution and Reaction Pathways in the Oxidative Degradation of CO_2-Loaded Aqueous MEA− MDEA Blends during CO_2 Absorption from Flue Gas Streams. Industrial & Engineering Chemistry Research. 2005 Feb 16;44(4):986-1003.
[21] Lawal AO, Idem RO. Kinetics of the oxidative degradation of CO_2 loaded and concentrated aqueous MEA-MDEA blends during CO_2 absorption from flue gas streams. Industrial & Engineering Chemistry Research. 2006 Apr 12;45(8):2601-7.
[22] Edali M, Aboudheir A, Idem R. Kinetics of carbon dioxide absorption into mixed aqueous solutions of MDEA and MEA using a laminar jet apparatus and a numerically solved 2D absorption rate/kinetics model. International Journal of Greenhouse Gas Control. 2009 Sep 1;3(5):550-60.
[23] Sema T, Naami A, Fu K, Edali M, Liu H, Shi H, Liang Z, Idem R, Tontiwachwuthikul P. Comprehensive mass transfer and reaction kinetics studies of CO_2 absorption into aqueous solutions of blended MDEA–MEA. Chemical Engineering journal. 2012 Oct 15;209:501-12.
[24] Adeosun A, El Hadri N, Goetheer E, Abu-Zahra MR. Absorption of $CO_2$by Amine Blends Solution: An Experimental Evaluation. International Journal of Engineering and Science. 2013;3(9):12-23.
[25] Naami A, Sema T, Edali M, Liang Z, Idem R, Tontiwachwuthikul P. Analysis and predictive correlation of mass transfer coefficient KGav of blended MDEA-MEA for use in post-combustion CO_2 capture. International Journal of Greenhouse Gas Control. 2013 Nov 1;19:3-12.
[26] Koronaki IP, Prentza L, Papaefthimiou V. Modeling of CO_2 capture via chemical absorption processes− An extensive literature review. Renewable and Sustainable Energy Reviews. 2015 Oct 1;50:547-66.
[27] Heydarifard M, Pashaei H, Ghaemi A, Nasiri M. Reactive absorption of CO_2 into Piperazine aqueous solution in a stirrer bubble column: Modeling and experimental. International Journal of Greenhouse Gas Control. 2018 Dec 1;79:91-116.
[28] Majeed H. Reactive absorption of CO_2 in single and blended amine systems. [Master's thesis]. Trondheim: Institutt for Kjemisk Prosessteknologi; 2013.

[29] Kierzkowska-Pawlak H. Determination of kinetics in gas-liquid reaction systems. An overview. Ecological Chemistry and Engineering S. 2012 Jan 1;19(2):175-96.
[30] Hogendoorn JA, Bhat RV, Kuipers JA, Van Swaaij WP, Versteeg GF. Approximation for the enhancement factor applicable to reversible reactions of finite rate in chemically loaded solutions. Chemical Engineering Science. 1997 Dec 1;52(24):4547-59.
[31] Hoftyzer PJ, Van Krevelen DW. Applicability of the results of small-scale experiments to the design of technical apparatus for gas absorption. InTransactions of the Institution of Chemical Engineers, Supplement (Proceedings of the Symposium on Gas Absorption 1954 (Vol. 32, pp. S60-S67).
[32] Last W, Stichlmair J. Determination of mass transfer parameters by means of chemical absorption. Chemical Engineering & Technology. 2002 Apr;25(4):385-91.
[33] Wenmakers PW, Hoorn JA, Kuipers JA, Deen NG. Gas–liquid mass transfer enhancement by catalyst particles, a modelling study. Chemical Engineering Science. 2016 May 12;145:233-44.
[34] Hikita H. Gas absorption with (m, n)-th order irreversible chemical reaction. International Chemical Engineering. 1964;4:332-40.
[35] Li X, Zhu C, Lu S, Ma Y. Mass transfer of SO2 absorption with an instantaneous chemical reaction in a bubble column. Brazilian Journal of Chemical Engineering. 2013 Sep;30(3):551-62.
[36] Alhseinat E, Mota-Martinez M, Peters C, Banat F. Incorporating Pitzer equations in a new thermodynamic model for the prediction of acid gases solubility in aqueous alkanolamine solutions. Journal of Natural Gas Science and Engineering. 2014 Sep 1;20:241-9.
[37] Sun WC, Yong CB, Li MH. Kinetics of the absorption of carbon dioxide into mixed aqueous solutions of 2-amino-2-methyl-l-propanol and piperazine. Chemical Engineering Science. 2005 Jan 1;60(2):503-16.
[38] Awais M. Determination of the mechanism of the reaction between CO_2 and alkanolamines [Master's thesis] Trondheim: Institutt for Kjemisk Prosessteknologi; 2013.
[39] Etemad E, Ghaemi A, Shirvani M. Rigorous correlation for CO_2 mass transfer flux in reactive absorption processes. International Journal of Greenhouse Gas Control. 2015 Nov 1;42:288-95.
[40] Pashaei H, Ghaemi A, Nasiri M. Modeling and experimental study on the solubility and mass transfer of CO 2 into aqueous DEA solution using a stirrer bubble column. RSC Advances. 2016;6(109):108075-92.
[41] Sadegh N, Stenby EH, Thomsen K. Acid gas removal from natural gas with alkanolamines: a modeling and experimental study. Kgs. Lyngby: Technical University of Denmark. 2013.
[42] Faramarzi L, Kontogeorgis GM, Thomsen K, Stenby EH. Extended UNIQUAC model for thermodynamic modeling of CO_2 absorption in aqueous alkanolamine solutions. Fluid Phase Equilibria. 2009 Aug 25;282(2):121-32.
[43] Sadegh N, Stenby EH, Thomsen K. Thermodynamic modeling of CO_2 absorption in aqueous N-Methyldiethanolamine using Extended UNIQUAC model. Fuel. 2015 Mar 15;144:295-306.
[44] Sanchez IC, Svendsen HF. Carbon dioxide solubility and mass transfer in aqueous amines for carbon capture. [Doctoral dissertation]. Austin: University of Texas; 2015.
[45] Lagarias JC, Reeds JA, Wright MH, Wright PE. Convergence properties of the Nelder--Mead simplex method in low dimensions. SIAM Journal on Optimization. 1998;9(1):112-47.
[46] Puxty G, Rowland R, Attalla M. Describing CO_2 mass transfer in amine/ammonia mixtures—No shuttle mechanism required. Energy Procedia. 2011 Jan 1;4:1369-76.
[47] Samanta A, Bandyopadhyay SS. Absorption of carbon dioxide into piperazine activated aqueous N-methyldiethanolamine. Chemical Engineering Journal. 2011 Jul 15;171(3):734-41.